Journal of Applied Polymer Science

Effect of rubber interparticle distance distribution on toughening behavior of thermoplastic polyolefin elastomer toughened polypropylene

Mohammad Fasihi, Hossein Mansouri
School of Chemical Engineering, Iran University of Science and Technology, Tehran 16846-3114, Iran
Correspondence to: M. Fasihi (E-mail: mfasihi@iust.ac.ir)

ABSTRACT: In this study, a blend of polypropylene (PP) and two types of thermoplastic polyolefin elastomers (TPO) were prepared by melt mixing. The TPOs were either ethylene- or propylene-based copolymer. The mechanical response and morphology of the blends were investigated using tensile and impact tests and scanning electron microscopy technique. There was significant increase in the impact strength of the TPO-modified PP, which was an outcome of fine dispersion of TPO inclusions. In particular, the blends containing PP-based TPO exhibited dramatic enhancement in toughness energy as featured by a plastic deformation in tensile test. The brittle-tough transition had several deviations from theoretical models, in which generally the interparticle distance criterion was realized as a single parameter, only controlled the transition of brittle to tough behavior. Moreover, the brittle-tough transition in tensile and impact mode tests was not coincident in the blend with a broad distribution of interparticle distance. © 2016 Wiley Periodicals, Inc. J. Appl. Polym. Sci. **2016**, *133*, 44068.

KEYWORDS: blends; morphology; mechanical properties

Received 5 July 2015; accepted 7 June 2016
DOI: 10.1002/app.44068

INTRODUCTION

Polypropylene (PP) is one of the most important and widely used polyolefins. It possesses outstanding properties such as easy processability, recycling ability and suitable heat stability, and also low cost. However, it has poor impact strength and therefore requires toughening up for many applications.

PP is commonly toughened by blending it with elastomers, such as ethylene–propylene rubber (EPR),[1,2] ethylene–propylene diene monomer (EPDM)[3–5] or with other thermoplastics like polybutene-1,[6,7] ethylene-1-hexene copolymer, or thermoplastic elastomers.[8–12] These blends are rarely miscible and often form a multiphase morphology.[1–8,13] The most important commercially produced blend, with the sole aim of toughening PP is PP/EPDM which normally exhibits more than 10 times higher impact strength and elongation to break than neat PP.[14,15] But substantial impact modification is just obtained by proper dispersing and vulcanizing of the rubber phase.[5,15] Several difficulties associated with producing this blend, such as fine dispersing of rubber phase and controlling the vulcanization process, resulted in more efforts to develop new alternative blends. In this field of research, thermoplastic elastomers have recently attracted much attention as a substitute for traditional rubbers because they possess comparable properties to thermoset rubbers, without requiring any compounding or vulcanization process.[7,8,16]

Thermoplastic polyolefin elastomers (TPO) are one of the most important group of thermoplastic elastomers which are typically based on polyethylene or PP or their copolymers, having long side chains grafted into the main chain. The crystalline domains in their structure act as physical junctions, playing a role similar to chemical crosslinks in vulcanized rubbers. Some types of TPO have been produced by commercial companies, using metallocene catalysts, such as Vistamaxx™ by ExxonMobil, propylene-based TPO, and Tafmer™ DF by Mitsui, ethylene-based TPO. The microstructure and properties of the TPOs modified PP studied previously in various works and high impact modification were reported.[17–19]

Apart from the experimental works on toughening of thermoplastics, various theoretical researches over the years tried to discover a criterion for brittle to tough transition in rubber-modified plastic blends. One of the well-known models was developed by Wu, based on experimental observations.[20,21] He introduced the interparticle distance or ligament thickness as a key parameter entirely controlling the brittle-tough transition. He observed that brittle-tough transition occurred at a critical value of interparticle distance which was an intrinsic

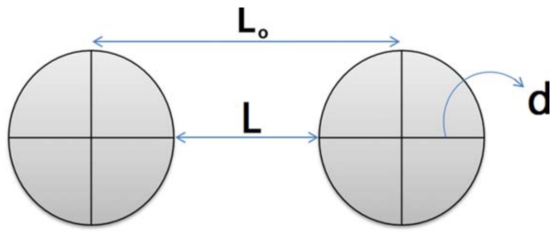

Figure 1. Schematics of rubber particles and interparticle distance. [Color figure can be viewed in the online issue, which is available at wileyonlinelibrary.com.]

characteristic of any matrix. But that notwithstanding, some recent researches knew rubber particle diameter and its volume fraction as among the most important parameters affecting the fracture behavior of polymer blends.[22,23]

Although some research works have been carried out on the toughening of PP by using TPOs, there exists no comparative study between the performances of ethylene- and propylene-based TPOs for toughening of PP. In addition, the capability of the theoretical models in the prediction of brittle-tough transition has not been considered in a blend with a wide distribution of interparticle distance. In this work, two kinds of toughened PP were prepared using ethylene- and propylene-based TPOs. The mechanical properties and phase morphology of these blends were investigated comparatively. Furthermore, the experimental brittle-tough transition was compared with theoretical models and some deviations were discussed.

BACKGROUND THEORY

Although there exists a correlation between rubber concentration and toughness, rubber content is not the main parameter which controls the toughness of the blend. Some models and theories have been proposed by various researchers to explain the key parameters controlling brittle to tough transition.[21,23,24] Wu was the first to demonstrate that toughness of such systems depends neither on rubber particle size nor on rubber concentration alone, but correlates with the interparticle distance or ligament thickness, which is related to both rubber particle size and its concentration. Interparticle distance or ligament thickness is defined as a surface to surface distance between two nearest neighbor particles, which is identified by "L" in Figure 1. He estimated this distance for uniform size and simplified well-dispersed particles using a lattice model according to the following equation[21]:

$$L=d\left[\left(\frac{\pi}{6\phi}\right)^{1/3}-1\right] \tag{1}$$

where L is the interparticle distance, d is the particle diameter, and ϕ is the particle volume concentration. Wu in his pioneering work on a rubber modified PA66 discovered that a sharp brittle–tough transition occurred when the interparticle distance, L, was smaller than a certain critical value, L_c. This critical value is an intrinsic characteristic of any matrix. Wu obtained L_c as being equal to 0.3 μm for PA66.[21] Some other researches introduced the value of 0.42 μm for PP.[25]

To take the distribution of rubber size into account, Wu proposed the following equation with the assumption of a log-normal distribution of the rubber particle size[21]:

$$L=d\left[\left(\frac{\pi}{6\phi}\right)^{1/3}-1\right]\exp\left(\ln^2\sigma\right) \tag{2}$$

here d is number-average diameter of rubber particles. After a while, Liu *et al.* derived a more accurate equation for calculating the interparticle distance in a polydisperse blend as follows[26]:

$$L=d\left[\left(\frac{\pi}{6\phi}\right)^{1/3}\exp\left(1.5\ \ln^2\sigma\right)-\exp\left(0.5\ \ln^2\sigma\right)\right] \tag{3}$$

In which σ is the particle size distribution parameter and can be calculated using the formula:

$$\ln\ \sigma=\sqrt{\frac{\sum_{i=1}^{N} n_i(\ln\ d_i-\ln\ d)}{\sum_{i=1}^{N} n_i}} \tag{4}$$

For monodisperse morphology, σ is equal to 1 and for polydisperse morphology, σ is greater than 1. It was discovered from eqs. (2) and (3) that an increase in the particle size distribution parameter (σ) resulted in a rapid increase in the interparticle distance. Thus, monodisperse particles bring more efficiency than polydisperse particles in rubber toughening. However, in all models, it was assumed that the interparticle distance was identical for every inclusion in the blend and its distribution was not considered at all.

EXPERIMENTAL

Materials

Commercial isotactic homopolypropylene (RG1102, Regal Petrochemical Co., Iran) with the melt flow index of 1 g/10 min was used as a polymeric matrix. Ethylene-based TPO, TPO1, (Tafmer DF 840, Mitsui Co., Japan) with a melting point of 58 °C and propylene-based TPO, TPO2, (Vistamaxx 6102, ExxonMobil Chemical Co., Irving, Texas, USA) with a melting point of 109 °C were used as toughening agents.

Samples Preparation

Binary blends were prepared by melt compounding of PP and each of toughening agents in a batch melt mixer (Brabender W50 EHT) for 10 min. The rotation speed and processing temperature were set at 80 rpm and 190 °C, respectively. The

Table I. Nomenclature and Composition of Samples

TPO2 (wt %)	TPO1 (wt %)	PP (wt %)	Sample
0	0	100	PP
0	5	95	PD5
0	10	90	PD10
0	15	85	PD15
0	20	80	PD20
5	0	95	PV5
10	0	90	PV10
15	0	85	PV15
20	0	80	PV20

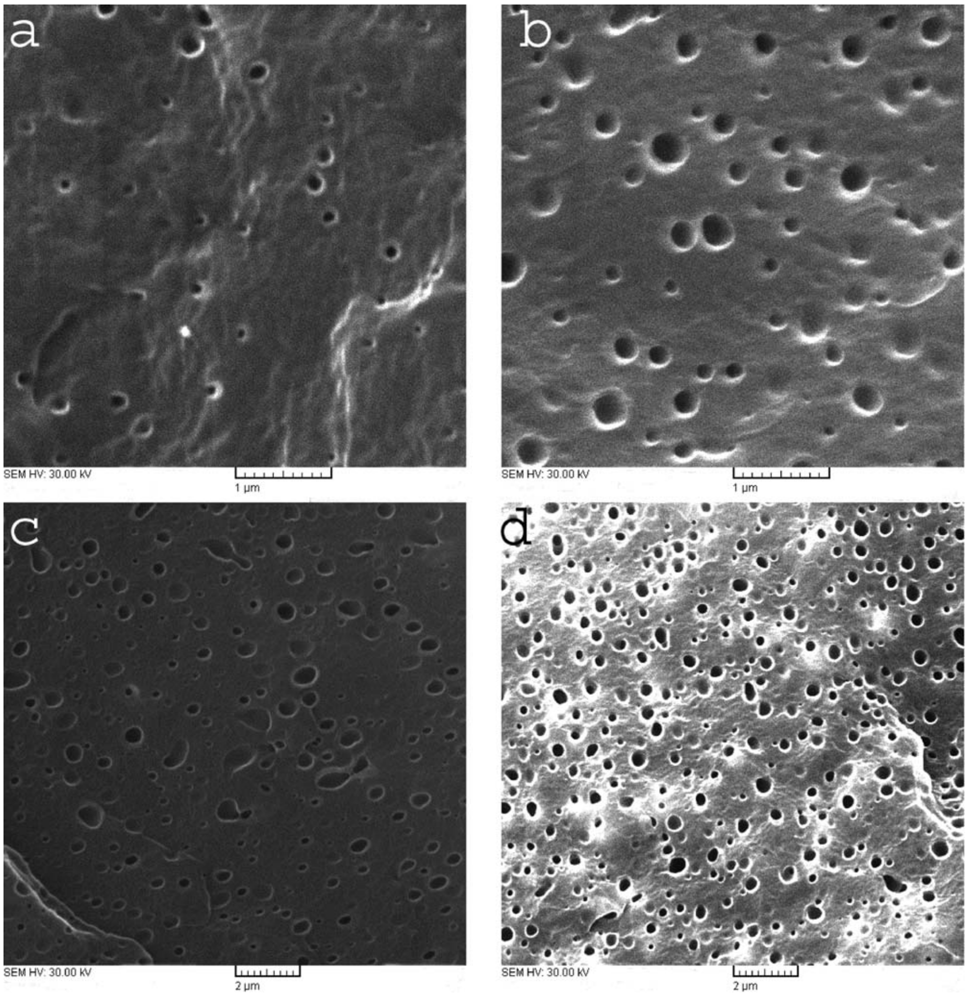

Figure 2. SEM micrographs of (a) PV5, (b) PV10, (c) PV15, and (d) PV20.

concentration of the toughening agent ranged from 5 to 20 wt %. For comparison, neat PP was processed at the same condition as well. The samples nomenclatures and compositions are listed in Table I.

After the melt compounding, all samples were compression-molded at 200 °C for 10 min and subsequently, cooled to room temperature by cold water circulation in about 12 min. A suitable mold was used to prepare standard dumbbell-shaped and ribbon-shaped bars for tensile and Izod impact tests, respectively.

Characterization Methods

The morphologies of the blends were observed by using scanning electron microscopy (SEM, VegaIITescan). For this purpose, the samples were fractured in liquid nitrogen followed by etching in n-heptane for 2 h in order to dissolve TPO inclusions. Prior to SEM characterization, a thin coating of gold was applied to the surface of samples in order to improve the image resolution. The size of the TPO inclusions and interparticle distance was then determined by analyzing the SEM images, using the ImageJ software program.

The complex viscosity of the components was measured as a function of frequency using rheometrics mechanical spectrometer (RMS Paar Physica US200) at 190 °C and strain amplitude of 1%.

Notched-Izod impact tests were conducted in accordance with ASTM D256 standard at room temperature, with a notch depth of 2.5 mm, using a U-F impact tester (Ueshima Seisakusho Ltd., Japan).

Tensile tests were conducted according to ASTM D 638 standard (Type I specimen, 50 mm gauge length, 12.7 mm width, and 4 mm thickness) at a crosshead speed of 50 mm/min using Universal Testing Machine (N-42, Gotech, Taiwan).

The obtained values of the tensile and Izod tests were averaged over at least four measurements.

RESULTS AND DISCUSSION

Investigation of Morphology

SEM images of the etched samples were recorded at different magnification with the aim of assessing the extent of TPO dispersion. Figure 2 displays the morphology of PP/TPO2 blends at different TPO concentration. A comparison between PP/TPO1 and PP/TPO2 blends at the same TPO content is also

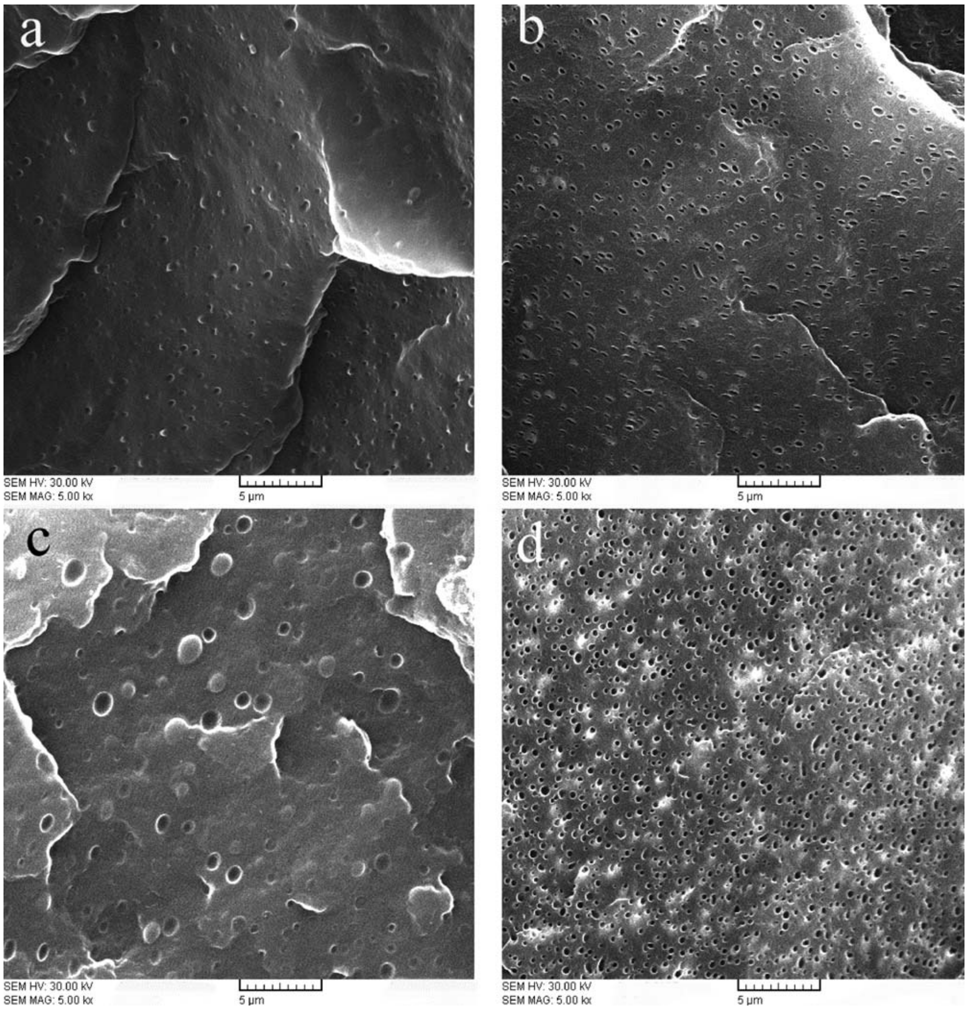

Figure 3. SEM micrographs of (a) PD10, (b)PV10, (c) PD20, (d)PV20.

presented in Figure 3. All blends exhibited phase separation of components in which TPO inclusions were the dispersed phase. The diameter of TPO particles in the blends varied from diameters less than 100 nm up to about 1 μm. TPO particles were mostly spherical but some ellipses were observed, especially at higher TPO concentration. The distribution and number of average sized TPO particles in different blends were estimated using ImageJ software and are expressed in Figures 4 and 5. The average inclusion diameter in the blends made by PP-based TPO (TPO2) were generally less than another type due to the probable lower interfacial tension and better adhesion between phases in this kind of blend. The average rubber sizes were 140 and 270 nm for PV5 and PD5, respectively. Although the conditions of mixing (shear rate, time, and Temperature) and interaction of matrix and rubber were identical in the blends produced by each type of TPOs, however, TPO particle size slightly increased as TPO concentration increased due to the higher possibility of rubber particle coalescence at the blends with higher rubber concentration.[27] An increase in the TPO content up to 15 wt % resulted in a slight increase in the average inclusions. The average size of TPO2 inclusions was always about 100–150 nm less than TPO1 in the same TPO concentration. However, the average inclusion size of PD20 had a sharp enhancement by about 100% upturn in comparison with PD15 due to more coalescence in the blend containing higher rubber concentration.[27–29]

In practice, it is not easy to measure the interfacial tension. However, it is possible to obtain a rough estimation of interfacial tension for two kinds of blends based on literature. Wu prepared some different polymer blends with 15 wt % of dispersed phase in a twin screw extruder and obtained a correlation between the capillary number and viscosity ratio of polymer blends as follows[30]:

$$\frac{\eta_m \dot{\gamma} d}{\sigma} = 4P^{\pm 0.84} \tag{5}$$

where η_m is the viscosity of the matrix, $\dot{\gamma}$ is the shear rate, d is the number-average particle diameter, σ is the interfacial tension and $P = \eta_d/\eta_m$ is the viscosity ratio in which η_d is the viscosity of dispersed phase. The plus (+) sign of the exponent applies for $P > 1$ and the minus (−) sign applies for $P < 1$. Equation (5) was also applied to polymer blends prepared in an internal mixer and gave reasonable results because the blends

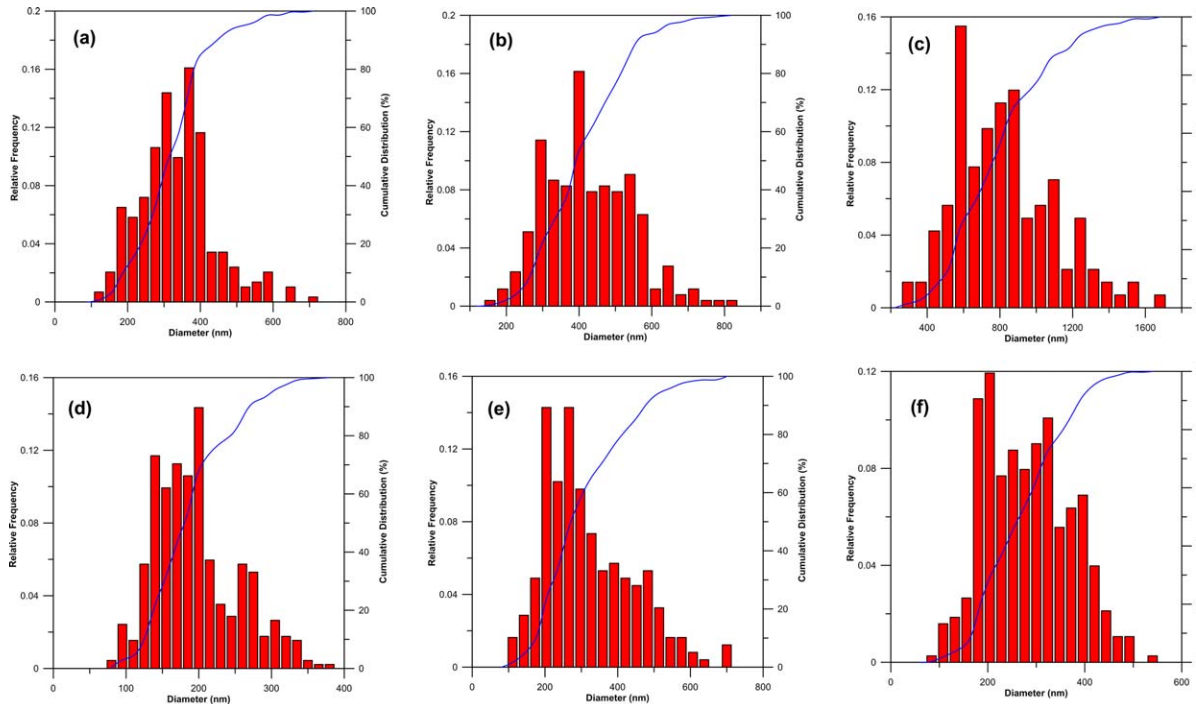

Figure 4. Histograms of TPO particle sizes in (a)PD10, (b)PD15, (c)PD20, (d)PV10, (e) PV15 and (f)PV20. [Color figure can be viewed in the online issue, which is available at wileyonlinelibrary.com.]

from the internal mixer had a morphology similar to that obtained from extruders.[31–33] This equation does not predict the dependence of d on the volume fraction of dispersed phase. In fact, this dependency was a result of rubber particle coalescence. So, this equation was applied to the blends with 5–15 wt % TPO and the average value for each type of blend was determined. To calculate the mixing shear rate in an internal mixer, Bousmina proposed a simple equation as follows[34]:

$$\dot{\gamma} = \frac{2\pi N}{\ln\left(R_e/R_i\right)} \tag{6}$$

where N is the rotation speed, R_i is the effective internal radius, and R_e is the external radius. R_i is a universal quantity for any internal mixer with a small gap between two rotors. To calibrate the internal mixer and determine the value of R_i, at least the rheological data of one polymer is required. The procedure of calibration was summarized in the previous study.[34] The obtained value for R_e/R_i was 1.10. The calculated shear rate for

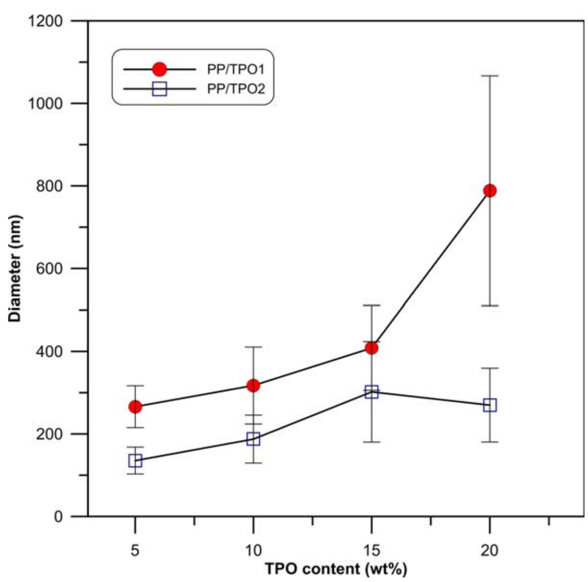

Figure 5. Number-average diameter of particles as a function of TPO content. [Color figure can be viewed in the online issue, which is available at wileyonlinelibrary.com.]

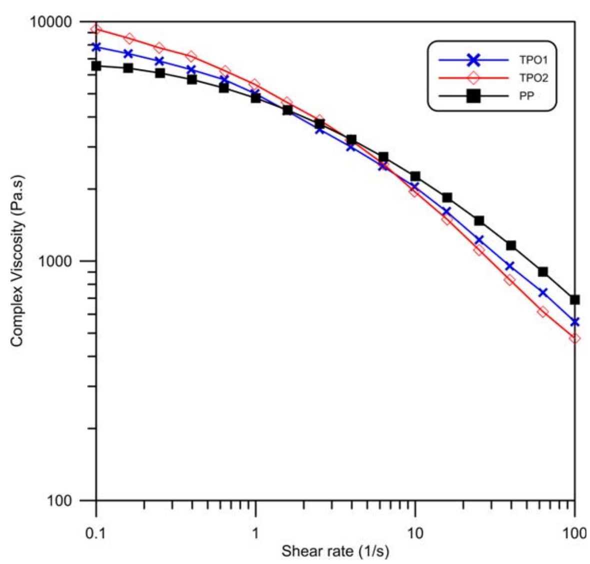

Figure 6. Complex viscosity of the components as a function of shear rate. [Color figure can be viewed in the online issue, which is available at wileyonlinelibrary.com.]

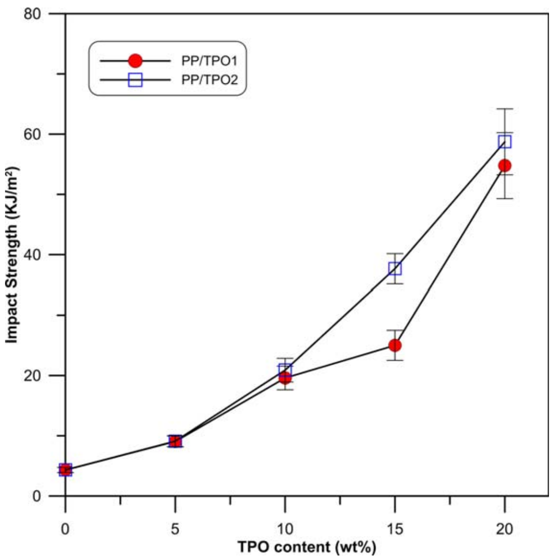

Figure 7. Impact strength of the blends as a function of TPO content. [Color figure can be viewed in the online issue, which is available at wileyonlinelibrary.com.]

applied mixing speed was 87 s^{-1}. The shear viscosity of the PP at $\dot{\gamma}$=87 s^{-1} and 190°C was obtained by rheometry and was equal to 720 Pa s. The viscosity ratio at the mentioned shear rate was got from the viscosity curve of components which is displayed in Figure 6. This ratio for PP/TPO1 was 0.78 and for PP/TPO2 was 0.67. Accordingly, the average interfacial tension of PP/TPO1 and PP/TPO2 blends were estimated to be 2.82 ± 0.53 and 1.74 ± 0.69 mN/m, respectively. The low values of interfacial tensions are evidences to ensure good adhesion between PP and TPOs. However, the lower interfacial tension of PP/TPO2 results in a better adhesion between phases in this type blend.

Impact Strength

Figure 7 presents the notched Izod impact strengths of the TPO modified PP blends. The impact strength of PP demonstrated a dramatic rise when modified with either type of TPO as a result of good adhesion between PP and rubber phases. Moreover, PP modified with TPO2 demonstrated higher impact strength than with TPO1 at the same weight percent of the rubber. The incorporation of 20 wt % TPO2 into the PP matrix enhanced its impact strength by more than 13 times. This value is well above the impact strength of commercial vulcanized PP/EPDM blends.[35,36]

The transition from brittle to tough behavior due to an increase in TPO content occurred gradually in our investigations, especially for PP/TPO1 blend, whereas theoretical models predict a sharp tough-brittle transition at a critical interparticle distance for rubber modified plastics. This kind of transition was supposed to be from a wide distribution of interparticle distance. As seen previously in the SEM images (Figure 3), in PP/TPO1 blends, interparticle distance varied in a wide range of value. The wide distribution of interparticle distance, presumably led to locally heterogeneous behavior in the regions with lower and upper interparticle distance than L_c. Thus, the transition from brittle to tough behavior occurred gradually. Although, some theoretical and experimental researches focused on determining the effect of the particle size distribution on tough-brittle transition, no special work has been performed yet on the influence of the distribution of interparticle distance to the best of our knowledge.

The distribution of interparticle distance in different blends measured from SEM images was obtained by measuring at least 200 individual interparticle distances. This distance was obtained by measuring the distance between a particle and its closest neighbor in the SEM images.[21]It should be note that the measured L from SEM micrograph is not identical with the shortest interparticle distance in three-dimensional sample. However, 3D measurement of L is not possible with the current equipment. The interparticle distance distributions of the blends are shown in the histograms in Figure 8. The results of the experimentally measured (by SEM image) and theoretically calculated [by the eq. (3)] average interparticle distance, L, are reported in Table II. The "*%L blow* L_c" in Table II was obtained from Figure 8 by determining the percent of measured L below 420 nm. The comparison between the measured and the calculated average L showed a high difference (about 25–50%) for the blends containing 5 and 10% TPOs and a minor difference (about 5–22%) for the higher TPO content blends. Furthermore, the measured data had a high standard deviation, especially for PP/TPO1 blend, which was attributed to the broad distribution of interparticle distance in this type of blend. PD20, in which the mean interparticle distance was higher than L_c (L_c for PP got from the literature equal to 420 nm[25]), expressed a tough behavior in impact test whereas just about 36% of inclusions had an interparticle distance lower than L_c. However, to uncover the quantitative contribution of interparticle distance distribution to the toughness modification, more research and experimental data are required.

Tensile Properties

The tensile stress-strain curves of the PD/TPO1 and PP/TPO2 blends are shown in Figure 9. As clearly seen, an increase in the rubber content resulted in a steady decrease in the tensile modulus and strength while elongation at break increased. Among all samples, PV15 and PV20 demonstrated advanced elongation at break with respectively more than 800% and 1500% improvement compared to the neat PP. It should be noted that the value of ultimate elongation at break, particularly for the sample with a high elongation at break (like PV15 and PV20), are merely estimates, since determinations were performed based on overall machine displacement. For these samples, the elongations were lower limits. The tensile properties of the blends determined from the stress–strain curves are presented in Table III. Tensile modulus and strength in either type of modified PP decreased linearly versus TPO content as depicted by the trends in Figure 10. The decline in these properties of the PP/TPO2 blends was associated with a steeper slope. The results demonstrated that incorporating 20 wt % of TPO1 and TPO2 into PP matrix caused respectively, a decrease in tensile modulus by 30 and 44% and tensile strength by 28 and 32%, relative to the unmodified PP. In contrast, ultimate elongation at break of the blends was higher than that of PP. In particular, by developing

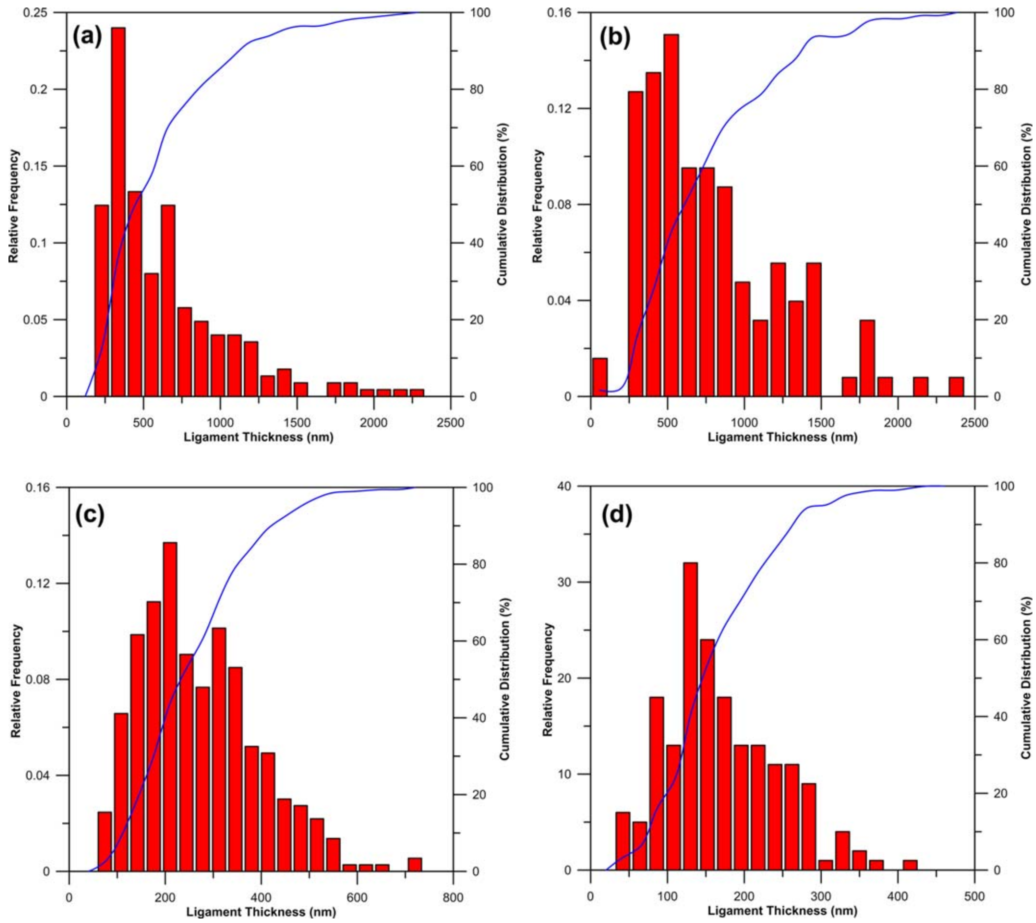

Figure 8. Histograms of ligament thickness in (a) PD10, (b) PD20, (c) PV10 and (d) PV20. [Color figure can be viewed in the online issue, which is available at wileyonlinelibrary.com.]

a high plastic deformation in the samples containing 15 and 20 percent TPO2 (i.e., PV15 and PV20), the toughness energy obtained from the area underneath the stress–strain curve was enhanced by 4.5 and 8.5 times in comparison with the neat PP, respectively. On the other hand, although PD20 had a high impact strength and tough behavior in impact loading, its elongation at break and consequently its toughness energy in tensile test experienced a minor modification. It should be noted that a considerable portion of interparticle distances in PD20 was greater than L_c, whereas in PV15, about 90% and in PV20 about 100% of them were lower than L_c.

There exist a few reports which introduce the relation between different toughness definitions like tensile testing toughness and

Table II. The Values of Calculated and Measured Interparticle Distance

Sample code	Mean diameter (nm)	Calculated $(L)^a$	σ	Measured (L)	Standard deviation	% L below L_c (420 nm)
PD5	266	363	1.28	477	317	54.0
PD10	318	738	2.01	589	389	44.2
PD15	408	540	1.81	576	379	47.6
PD20	789	478	1.43	610	390	36.3
PV5	136	186	1.29	364	191	67.0
PV10	187	178	1.36	255	120	90.2
PV15	302	238	1.50	251	136	88.9
PV20	270	160	1.42	191	93	100

[a] Calculated by eq. (3).

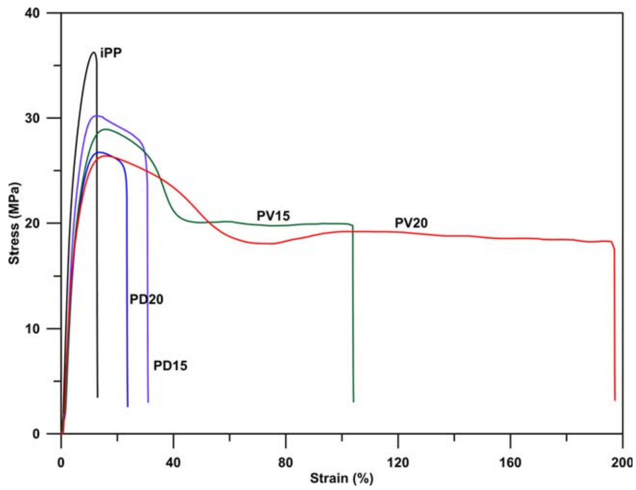

Figure 9. Stress-strain curves of samples. [Color figure can be viewed in the online issue, which is available at wileyonlinelibrary.com.]

toughness determined in impact testing. Brostow et al. expressed a mathematical relationship between the impact energy and the brittleness for some polymers and other materials based on experimental observations.[37] The brittleness (B) was defined quantitatively as:

$$B=\frac{1}{\varepsilon_b E'} \tag{9}$$

where $\mathring{a}_b$ is the tensile elongation at break and E' is the storage modulus determined by dynamic mechanical analysis (DMA). On the other hand, an inverse relationship between brittleness and tensile toughness in a separate study was also developed.[38] Given the outcome of the two works, it should be a direct relation between Izod impact energy and tensile toughness. However, they just considered the properties of pure polymers, but not blends or composites. Moreover, the goodness of fit parameter of the equation offered by Brostow et al. for Izod impact energy was so low ($R^2 = 0.7$).[37] So, it cannot be expected to have a direct relation between Izod impact energy and tensile toughness for every kind of polymer (e.g., polymer blends).

A comparison between brittle-tough transition in impact and tensile tests of the blends revealed that in the blend having a

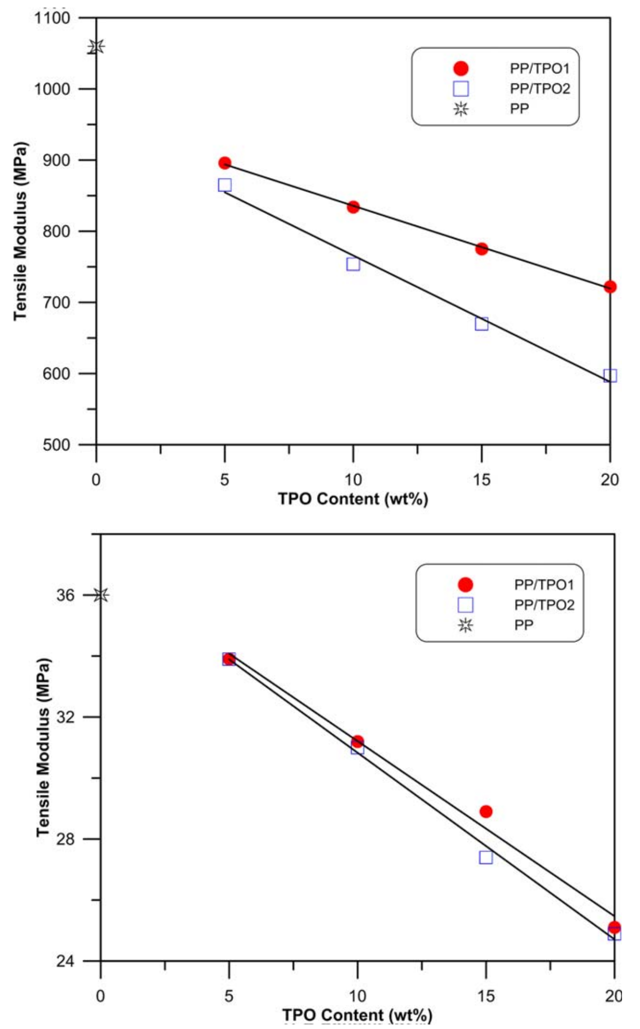

Figure 10. Tensile modulus and tensile strength as a function of TPO content. [Color figure can be viewed in the online issue, which is available at wileyonlinelibrary.com.]

good distribution of rubber inclusion (PP/TPO2), the transition to tough behavior occurred simultaneously in tensile and impact tests as PV20 which exhibited tough behavior in either impact or tensile test. While in another type of blend

Table III. Tensile and Impact Properties of Blends

Sample code	Young's modulus (MPa)	Elongation at break (%)	Tensile strength (MPa)	Toughness energy (kJ)	Impact strength (kJ/m^2)
PP	1,060	13	36.0	12.7	4.3
PD5	896	30	33.9	24.1	9.1
PD10	834	32	31.2	19.8	17.5
PD15	775	32	28.9	19.6	37.7
PD20	722	24	25.1	14.8	54.8
PV5	865	23	33.9	16.0	9.1
PV10	754	25	31.0	15.4	20.9
PV15	670	109	27.4	57.5	37.7
PV20	597	198	24.9	108.5	58.7

(PP/TPO1) having a poor distribution of rubber inclusion, the transitions from brittle to tough behavior were not coincident in tensile and impact mode tests. As PD20, having a tough behavior in the impact test, displayed a brittle behavior in the tensile test. Because in PV20 almost all inclusions had lower interparticle distance than L_c, but in PD20 just 36% had that feature. It seems that the sensitivity of tensile test mode to the mean and distribution of interparticle distance is higher than impact test because in tensile testing, actually, all the points of the material respond to the tensile stress and local brittleness in any region may cause the sample to fail.

CONCLUSIONS

In this study, PP was blended with either ethylene- or propylene-based TPO, and subsequently microstructure and mechanical properties of the blends were investigated. Propylene-based TPO formed a finer dispersed morphology with a relatively narrow interparticle distance distribution. In this case, by incorporating 20 wt % TPO, impact strength and toughness energy of PP was enhanced up to 13 and 8.5 times, respectively, and the brittle-tough transition was in agreement with Wu's model. Furthermore, a parallel brittle-tough transition in tensile and impact test was observed in propylene-based TPO, while the blend containing ethylene-based TPO with a broad distribution of interparticle distance showed similar improvement in impact strength but none with tensile energy. Non-simultaneous brittle-tough transition in tensile and impact loading in ethylene-based TPO blends was attributed to the wide distribution of interparticle distance. In fact, in tensile testing, all the points of the material respond to the tensile stress and local inhomogeneity in any region may cause the sample to fail.

ACKNOWLEDGMENTS

The authors would like to thank the Iran National Science Foundation (INSF) for the financial support of this study (grant number 92008345).

REFERENCES

1. D'Orazio, L.; Mancarella, C.; Martuscelli, E.; Sticotti, G. *Polymer* **1993**, *34*, 3671.
2. Mnif, N.; Massardier, V.; Kallel, T.; Elleuch, B. *Polym. Compos.* **2009**, *30*, 805.
3. Rondin, J.; Bouquey, M.; Muller, R.; Serra, C. A.; Martin, G.; Sonntag, P. *Polym. Eng. Sci.* **2014**, *54*, 1444.
4. Brostow, W.; Datashvili, T.; Hackenberg, K. P. *Polym. Compos.* **2010**, *31*, 1678.
5. Yeh, J. T.; Lin, S. C. *J. Appl. Polym. Sci.* **2009**, *114*, 2806.
6. Cham, P. M.; Lee, T. H.; Marand, H. *Macromolecules* **1994**, *27*, 4263.
7. Thomann, Y.; Suhm, J.; Thomann, R.; Bar, G.; Maier, R. D.; Mülhaupt, R. *Macromolecules* **1998**, *31*, 5441.
8. Yamaguchi, M.; Miyata, H.; Nitta, K. H. *J. Appl. Polym. Sci.* **1996**, *62*, 87.
9. Bai, H.; Wang, Y.; Song, B.; Li, Y.; Liu, L. *J. Polym. Sci. Part B: Polym. Phys.* **2008**, *46*, 577.
10. Wahit, M. U.; Hassan, A.; Ishak, Z. A. M.; Czigany, T. *eXPRESS Polym. Lett.* **2009**, *3*, 309.
11. Ichazo, M.; Hernandez, M.; Gonzalez, J.; Albano, C.; Dominguez, N. *Polym. Bull.* **2004**, *51*, 419.
12. Sengupta, P.; Noordermee, J. W. M. *J. Elastomers Plast.* **2004**, *36*, 307.
13. Yamaguchi, M.; Miyata, H. *Macromolecules* **1999**, *32*, 5911.
14. da Silva, A. L. N.; Coutinho, F. M. B. *Polym. Test.* **1996**, *15*, 45.
15. Taşdemir, M.; Topsakaloğlu, M. *J. Appl. Polym. Sci.* **2007**, *104*, 3895.
16. Grein, C.; Gahleitner, M.; Bernreitner, K. *Exp. Polym. Lett.* **2012**, *6*, 688.
17. Chen, X.; Ma, G.; Li, J.; Jiang, S.; Yuan, X.; Sheng, J. *Polymer* **2009**, *50*, 3347.
18. Tsou, A. H.; Lyon, M. K.; Chapman, B. R.; Datta, S. *J. Appl. Polym. Sci.* **2008**, *107*, 1362.
19. Mäder, D.; Thomann, Y.; Suhm, J.; Mülhaupt, R. *J. Appl. Polym. Sci.* **1999**, *74*, 838.
20. Wu, S. *Polymer* **1985**, *29*, 1855.
21. Wu, S. *J. Appl. Polym. Sci.* **1988**, *35*, 549.
22. Bucknall, C. B.; Paul, D. R. *Polymer* **2013**, *54*, 320.
23. Bucknall, C. B.; Paul, D. R. *Polymer* **2009**, *50*, 5539.
24. Corté, L.; Leibler, L. *Macromolecules* **2007**, *40*, 5606.
25. Wang, Y.; Fu, Q.; Qijun, L.; Gong, Z.; Shen, K.; Wang, Y. Z. *J. Appl. Polym. Sci.* **2002**, *40*, 2086.
26. Liu, Z. H.; Li, R. K. Y.; Tjong, S. C.; Qi, Z. N.; Wang, F. S.; Choy, C. L. *Polymer* **1998**, *39*, 4433.
27. Liu, Y.; Zhang, M.; Zhang, X.; Gao, J.; Wei, G.; Huang, F.; Song, Z.; Qiao, J. *Macromol. Symp.* **2003**, *193*, 81.
28. Saeb, M. R.; Khonakdar, H. A.; Moghri, M.; Razban, M.; Jazani, O. M.; Alorizi, A. E. *Polym. Plast. Technol. Eng.* **2014**, *53*, 1142.
29. Zare, Y.; Garmabi, H. *Appl. Surf. Sci.* **2014**, *321*, 219.
30. Wu, S. *Polym. Eng. Sci.* **1987**, *27*, 335.
31. Shariatpanahi, H.; Nazokdast, H.; Dabir, B.; Sadaghiani, K.; Hemmati, M. *J. Appl. Polym. Sci.* **2002**, *86*, 3148.
32. Shariatpanahi, H.; Nazokdast, H.; Hemmati, M. *J. Appl. Polym. Sci.* **2003**, *88*, 54.
33. Lin, B.; Sundararaj, U. *J. Appl. Polym. Sci.* **2004**, *92*, 1165.
34. Bousmina, M.; Ait-Kadi, A.; Faisant, J. B. *J. Rheol.* **1990**, *43*, 415.
35. Wang, W.; Wu, Q.; Qu, B. *Polym. Eng. Sci.* **2003**, *43*, 1798.
36. Gupta, N. K.; Jain, A. K.; Singhal, R.; Nagpal, A. K. *J. Appl. Polym. Sci.* **2000**, *78*, 2104.
37. Brostow, W.; Hagg Lobland, H. E. *J. Mater. Sci.* **2010**, *45*, 242.
38. Brostow, W.; Hagg Lobland, H. E.; Khoja, S. *Mater. Lett.* **2015**, *159*, 478.